

Nonlinear optoacoustic readings from diffusive media at near infrared wavelengths

Jaber Malekzadeh-Najafabadi^{1,§}, Jaya Prakash^{1,2,§}, and Vasilis Ntziachristos^{1,2,*}

*Corresponding author

Vasilis Ntziachristos, Ph.D., Professor:
Chair for Biological Imaging,
Technical University of Munich,
Ismaningerstraße 22, D-81675, Germany.
Telephone number: +49 89 3187 3852
Fax: +49 89 3187 3017
Email: v.ntziachristos@tum.de

¹Chair of Biological Imaging, Technical University of Munich, Ismaninger Straße 22, D-81675, Germany.

²Institute of Biological and Medical Imaging, Helmholtz Zentrum München, Ingolstaedter Landstraße 1, Neuherberg D-85764.

[§]Equal Contribution

Keywords: optoacoustic (photoacoustic) imaging, nonlinearity, optical parameters, optical imaging.

Abstract

Optoacoustic (photoacoustic) imaging assumes that the detected signal varies linearly with laser energy. However, non-linear intensity responses as a function of light fluence have been suggested in optoacoustic microscopy, i.e. within the first millimeter of tissue. In this work, we explore the presence of nonlinearity deeper in tissue (~4mm), as it relates to optoacoustic mesoscopy, and investigate the fluence required to delineate a switch from linear to non-linear behavior. Optoacoustic signal non-linearity is studied for different materials, different wavelengths and as a function of changes in the scattering and absorption coefficient of the medium imaged. We observe fluence thresholds in the mJ/cm^2 range and preliminary find that different materials may exhibit different non-linearity patterns. We discuss the implications of non-linearity in relation to image accuracy and quantification in optoacoustic tomography.

This article has been accepted for publication and undergone full peer review but has not been through the copyediting, typesetting, pagination and proofreading process, which may lead to differences between this version and the [Version of Record](#). Please cite this article as [doi: 10.1002/jbio.201600310](https://doi.org/10.1002/jbio.201600310)

1. Introduction

Optoacoustic imaging resolves optical contrast deep inside tissues at ultrasound resolution, thus offering high-resolution optical imaging [1-4]. Quantification of optoacoustic signals is important in characterizing tissue chromophores or administered agents and/or nano-particles. Typically studies in optoacoustic imaging assume that the detected signal amplitude varies linearly with the light fluence delivered on the sample. However, recent reports suggested nonlinear optoacoustic intensity readings in response to increasing light fluence on microscopic specimens [5-14]. Nonlinear signals have been collected from exogenous dyes, nanoparticles, and chromophores [5-8] and different mechanisms have been proposed responsible for the non-linear behavior, including the formation of nano-bubbles [5, 6], changes of thermo-physical parameters, such as thermal expansion coefficient, due to local temperature enhancement around particles at high laser fluence [9], saturation of the absorption coefficient [7] or evaporation of fluids surrounding heated particles (250-355 °C for water) [5]. It is understood that different phenomena may contribute to the generation of non-linear optoacoustic responses, depending on the amount of energy or power utilized and the medium interrogated.

Optoacoustic microscopy studies reported a linear increase in the signal strength with an increased concentration of nanoparticles and a nonlinear optoacoustic signal increase as a function of laser fluence [9]. Nonlinear signals have been employed in optoacoustic microscopy to differentiate single absorbing targets over an absorbing background, the latter generating weak linear responses [6]. The nonlinear change in the initial pressure rise was also considered for improving upon the acoustic diffraction limit [10] and for improving the lateral and axial resolution in optoacoustic microscopy [14].

While the dependence of non-linear phenomena on wavelength and concentration has been studied in the microscopic regime, the presence and characteristics of non-linearity in

optoacoustic mesoscopy [15] has not been so far investigated. Differently than optoacoustic microscopy that uses focused light beams, optoacoustic mesoscopy employs broad-beam illumination, which offers different light distribution patterns in diffusive media. Moreover, while microscopy operates at penetration depths of a few hundred micrometers [16], optoacoustic mesoscopy operates at depths of a few millimeters. Therefore mesoscopic optoacoustic imaging is based on different operational characteristics compared to microscopic techniques. For this reason, we aimed herein to investigate the presence of non-linear phenomena associated with diffusive light measurements and identify the characteristics of hypothesized transitions between linear and non-linear responses, which relates to emerging clinical application of optoacoustics. In addition, we performed a systematic study for understanding the dependence of non-linear responses on light fluence, within mesoscopic samples. We examine the responses of different optically absorbing substances, i.e. hemoglobin, ICG and India Ink and the non-linearity dependence on wavelength. We discuss how our observations may affect the performance and accuracy of optoacoustic tomography.

2. Results

Figure 1 depicts results that characterize the relationship between the light fluence and the optoacoustic signal detected at wavelength 800 nm. Figure 1(a) plots the raw optoacoustic signals collected from an agar absorber (MEAS-1) in response to light fluence ranging from 3.22 mJ/cm^2 to 22.59 mJ/cm^2 increasing in steps of 3.23 mJ/cm^2 . Figure 1(b) plots the absolute intensity of the signals as a function of light fluence at different depths of 0.75, 1.07, 1.91, and 4.2 mm, which correspond to time-points 23.5, 23.7, 24.3, and 25.8 μs in Figure 1(a), respectively. There is an initial linear response when the fluence is 0-8, 0-14, 0-16, and 0-23 mJ/cm^2 for depths of 0.75, 1.07, 1.91, and 4.2 mm, respectively. However higher fluence results in a nonlinear behavior for the depths of 0.75, 1.07, and 1.91 mm. Differences in the non-linearity observed can be explained by the decreasing light fluence with depth in

diffusive media. The response for the 4.2 mm depth is linear, which indicates that the light fluence reaching this depth is not sufficient for imparting non-linear effects. Figure 1(c) illustrates the differences in laser pulse width observed are small (~ 4 -5 ns). Therefore, the pulse width variation should not play a significant role in the results shown in Figure 1(b), because the stress relaxation time is typically much longer than a few nanoseconds. Hence stress confinement is expected to be similar with the different pulse widths [17].

Figure 2 shows the results of MEAS-2, which studied the effects of absorber concentration on the optoacoustic signal as a function of light fluence at wavelength of 800 nm. The detected optoacoustic signal exhibits prominent non-linearity with the increase of the absorption coefficient. Similar to the observation in Figure 1(b), all curves exhibit linear behavior for low fluence but a steeper ascend at higher fluence. At the upper part of light fluence employed we observe saturation effects. The nonlinearity here follows a piecewise linear function and the slope of second part of the piecewise linear function is bigger compared to first part of the function. In addition, as expected, higher absorption coefficient generates a stronger optoacoustic signal. Figure 2(a) depicts the raw signals, whereby Figure 2(b) shows the same curves as in Figure 2(a) but normalized to their maximum value.

Results from MEAS-3, employed to characterize the relationship of the optoacoustic signal (amplitude) to the scattering coefficient are shown in Figure 3. Figure 3(a) illustrates the nonlinear optoacoustic signal variation with increasing scattering coefficient and light fluence. A strong signal increase is observed for scattering media, compared to the non-scattering medium. Plotting the normalized profiles of the recorded signals exhibits that the optoacoustic signal in the non-scattering medium behaves linearly, whereby the signal trends for the scattering media are similarly non-linear. The result indicates that scattering-related modifications in diffusive media change the responses expected as a function of fluence, compared to non-scattering media. Figure 3(c) plots the raw optoacoustic signals recorded for the different scattering schemes examined. The amplitude of optoacoustic signal for the non-

scattering phantom is approximately an order of magnitude lower over the scattering medium, an observation that nevertheless depends on the divergence and spatial distribution characteristics of the illuminating beam employed. All measurements were done at 800 nm.

To interrogate the relation between the absorber material, light fluence and optoacoustic responses we measured different phantoms containing ICG, Hemoglobin and Ink, imparting the same absorption coefficient (MEAS-4), at the absence of scattering. Figure 4(a) depicts the signals collected from the three materials as a function of light fluence at wavelength 800 nm. It is clearly observed that the materials exhibit different non-linear responses. Ink follows a linear behavior, as demonstrated in Figure 3. However, hemoglobin shows a steeper initial increase, which then exhibits early saturation effects, evident on the normalized plot shown in Figure 4(b). ICG follows a response similar to hemoglobin. Figure 4(c) illustrates the result acquired from blood phantom, ICG phantom and ink phantom (only ink phantom had scattering, reduced scattering coefficient of 10 cm^{-1}). The response from the ink phantom confirms the observations in Figure 3. Figure 4(d) depicts the normalized plot of Figure 4(c) for better comparison of non-linearity in the three materials examined.

We also interrogated the optoacoustic signal collected from three phantoms of India ink and agar of the same absorption coefficient, by illuminating them at different wavelengths (MEAS-5). For each wavelength results from three consecutive measurements (1h apart) were normalized to maximum signal values (Figure 5). The results show different optoacoustic signal intensity trends as a function of wavelength. Optoacoustic signal attained saturation at 11 mJ/cm^2 at 700 nm, 12 mJ/cm^2 at 750 nm, and 13 mJ/cm^2 at 800 nm. These findings results may relate to energy difference of photons between wavelengths, since photons at lower wavelengths have higher energy.

3. Material and Methods

3.1. Experimental Setup

To interrogate the nonlinear optoacoustic phenomenon in the near infrared region with different diffuse samples and varying concentrations, we built a simple experimental arrangement (Figure 6). The laser in the experimental setup illuminates a cylindrical phantom located at the center of a circle region with 3.5 cm-diameter and 5 cm-height filled with water. A separation of 3.5 cm between phantom and laser was used to provide approximately uniform illumination on the sample. The focal length of the transducer used for data collection was 3.5 cm. Illumination comes from a tunable optical parametric oscillator (OPO) laser (InnoLas Laser GmbH). A two sided illumination (with Gaussian beam profile) was achieved by guiding the light with a four-branch fiber bundle (WF 179, NA: 0.22, tip-Diameter: 2.5mm, CeramOptec GmbH) onto the phantom. The other two fiber branches illuminate the optical sensor of a power meter (FieldmaxII-TOP, Coherent, CA, USA). To approximately calculate light fluence on the surface of phantom, the measured energy is divided by illumination area at sample location. Optoacoustic signals were detected using a single element ultrasound transducer (Olympus, PZT), with a central frequency of 3.5 MHz and a detector bandwidth of 90%. The signals were amplified (AU-1291 amplifier, L-3 Narda-MITEQ) and recorded using a data acquisition card (PCI-7340, NIC). For measurements, phantoms of 4.5 mm diameter were inserted at the center of the field of view.

3.2. *Material*

In this study, ink (Black India, Higgins, USA), Intralipid (20% emulsion, I141-100ML, SIGMA) and agar (05039-500G, Fluka, Spain) were used to prepare tissue mimicking phantoms. Ink was proportionally diluted by deionized water to have a phantom with a desired absorption coefficient, as determined by a spectrometer (LS-1-cal, USB4000, Oceanoptics, Germany). Different reduced scattering coefficient values were achieved by varying the concentration of the intralipid in the mixture [18]. Lastly, two percent agar was added to the solution and heated in a microwave oven.

3.3. Non-linear characterization

In a first measurement (MEAS -1) we examined generation of non-linear optoacoustic signals in diffusive materials. The signals were produced by a 4.5 mm-diameter cylinder made of a mixture of ink, Intralipid and agar having an absorption coefficient of 0.23 cm^{-1} and reduced scattering coefficient of 10 cm^{-1} at 800 nm. The raw optoacoustic signals were recorded and the maximum signal peak was plotted as a function of the different parameters examined. For control purposes, the laser pulse width at different laser energy was characterized after detecting the pulse by a high speed photodiode and an oscilloscope.

3.4. Effect of material concentration

In a second measurement (MEAS-2), we interrogated the optoacoustic signal generated as a function of the absorption coefficient of the medium. 4.5 mm agar cylinders were prepared containing different amounts of India ink at concentrations that yielded absorption coefficient values of 0.46 cm^{-1} (0.2 OD), 0.23 cm^{-1} (0.1 OD), and 0.11 cm^{-1} (0.05 OD) at the wavelength 800 nm. The reduced scattering coefficient in all cases was 10 cm^{-1} .

3.5. Effect of Scattering

In a third measurement (MEAS-3), the nonlinear optoacoustic effect was studied by increasing the optical reduced scattering coefficient in the phantom. Tissue mimicking agar cylinders of 4.5 mm –diameter were generated by adding a mixture of agar and ink (imparting optical absorption with 0.05 OD at 800 nm) and intralipid (for optical scattering). The reduced scattering coefficients tested were: 20 cm^{-1} , 15 cm^{-1} , 10 cm^{-1} . A control measurement was also obtained from a phantom that contained no scattering material.

3.6. Non-linearity of different materials

The nonlinear effect from different materials (ink, indocyanine green (ICG) and hemoglobin) was also studied (MEAS-4). 4.5 mm-diameter cylinders contained blood, ICG or India ink mixed with agar. The amount of absorbing material employed was adjusted so that

the absorption coefficient in the cylinders was $\mu_a = 0.23 \text{ cm}^{-1}$ at 800 nm, for all three materials studied. No scattering material was employed in the phantom, so that the effect of material is studied independently of scattering effects

3.7. *Measurements at different wavelengths*

To examine non-linear effects at different wavelengths, we prepared three 4.5 mm-diameter agar cylinders with different India Ink concentrations adjusted to yield the same absorption coefficient of 0.46 cm^{-1} at all wavelengths examined, i.e. 700 nm, 750 nm, and 800 nm. The three cylinders were then measured (MEAS-5) at the corresponding wavelengths they were prepared for. Each measurement was repeated 3 times. The phantoms in this case have no scattering to remove effect of scattering at different wavelengths.

4. Discussion

We have shown that non-linear effects can be observed in optoacoustic mesoscopy at light fluences that are typically employed for imaging purposes. Non-linearity was observed as a function of OD changes (absorption), scattering changes and in relation to the material and wavelength employed. The study was performed using absorbers of the same size, in order to decompose the observations from ultrasound frequency variation. All measurements were obtained at the same optoacoustic signal bandwidth. In addition, the same transducer and overall experimental arrangement was employed in all experiments, so our results are unlikely to reflect variations in transducer properties, such as central frequency, bandwidth or sensitivity field. The primary dependence of the effects observed on light fluence can be further corroborated by observing the raw optoacoustic signal collected as a function of time. For example, in Figure 1(b) the optoacoustic signal increased non-linearly at the 23.5 μs time point, but linearly at the 25.8 μs time point. Deeper-seated signals, collected at later time points, experience reduced light-fluence due to the attenuation of light propagating in the

medium and therefore may not be excited with energy that is sufficient to impart non-linear behavior.

The non-linear effects observed were not evident in non-scattering material (Figure 3). A possible explanation for this observation relates to the light propagation pattern inside the phantom. Since the distribution of light inside the non-scattering phantom follows propagation along diverging straight lines, the effective absorption cross-section and excitation energy deposited on the absorber is less than in diffusive light propagation, which allows multiple interactions between photons and the absorber. The non-linearity effects observed follows different trends in different materials, implicating involvement of the molecular nature of absorbers. Likewise, nonlinearity follows different trends at different wavelengths (i.e. Figure 5 at 700 nm, 750 nm and 800 nm) and may be associated with the different energy of photons at different wavelengths.

All measurements were performed by explicitly measuring the light fluence delivered to the phantom for each energy setting examined. Nevertheless there can be errors in the measurement of absolute light fluence measured. Moreover, there is a small dependence of the light pulse width to the energy of the pulse, which may also have a contribution to the results observed.

Our results suggest that conventional reconstruction algorithms for optoacoustic imaging, which assume linear behavior, may be less accurate at light fluence above a certain threshold. In our measurements this threshold was found to be $\sim 7 \text{ mJ}/\text{cm}^2$ which relies on measurement under the Maximum Permissible Exposure (MPE) limits [19]. The non-linearity observed was found in superficial layers at depths $< 2 \text{ mm}$ for our phantoms (Figure 1b), but the significance of the observed non-linearity extend to the entire image during reconstruction from collected optoacoustic data at mesoscopic scales. Since we reconstruct the entire field of view (both at the mesoscopic and macroscopic regimes), the dynamic range of the entire imaging domain will be affected due to observed non-linearity [20-23]. Therefore, it is

necessary to further investigate correction for the non-linear response to improve tomographic or spectral unmixing quantification when using pulses of higher energy. Future studies should examine additional factors that may contribute to non-linear optoacoustics. Generation of optoacoustic signal depends on more parameters of the medium, including the optical bulk modulus, specific heat capacity, and thermoelastic expansion coefficient; as well as numerous parameters of the measurement set-up, including detection frequency and acoustic attenuation.

Acknowledgements

This work was funded by the European Commission under Grant Agreement Number 605162, the European Union's Horizon 2020 research and innovation programme under grant agreement No 687866 (INNODERM), and the Deutsche Forschungsgemeinschaft (DFG) as part of the CRC 1123 (Z1). Jaya Prakash acknowledges Alexander von Humboldt Postdoctoral Fellowship program.

References

- [1] V. Ntziachristos, J. Ripoll, L. V. Wang, and R. Weissleder, *Nat. Biotechnology* 23, 313-320 (2005).
- [2] L. V. Wang, and S. Hu, *Science* 335, 1458-1462 (2012).
- [3] V. Ntziachristos, *Nat. Methods* 7, 603-614 (2010).
- [4] A. Taruttis, V. Ntziachristos, *Nat. Photonics* 9, 219-227(2015)
- [5] V. P. Zharov, *Nat. Photonics* 5, 110–116 (2011).
- [6] M. Sarimollaoglu, D. A. Nedosekin, Y. A. Menyaev, M. A. Juratli, and V. P. Zharov, *PACS* 2, 1-11 (2014).
- [7] A. Danielli, K. Maslov, C. P. Favazza, J. Xia, and L. V. Wang, *Appl. Phys. Lett.* 106, 203701 (2015).

- [8] A. Danielli, C. P. Favazza, K. Maslov, and L. V. Wang, *Appl. Phys. Lett.* 97, 163701 (2010).
- [9] S. Y. Nam, L. M. Ricles, L. J. Suggs, and S. Y. Emelianov, *Opt. Lett.* 37, 4708-4710 (2012).
- [10] P. Lai, L. Wang, J. W. Tay, and L. V. Wang, *Nat. Photonics* 9, 126-132 (2015).
- [11] E. Petrova, S. Ermilov, R. Su, V. Nadvoretzkiy, A. Conjusteau, and A. Oraevsky, *Opt. Express* 21, 25077-25090 (2013).
- [12] O. Simandoux, A. Prost, J. Gateau, and E. Bossy, *PACS* 3, 20-25 (2015).
- [13] C. S. Yelleswarapu, and S. R. Kothapalli, *Opt. Express* 18, 9020-9025 (2010).
- [14] D. A. Nedosekin, E. L. Salanzha, E. Dervishi, A. S. Biris, and V. P. Zharov, *Small* 10, 135-142 (2015).
- [15] Aguirre et al, *Nat. Biomedical Engineering* 1, 0068 (2017)
- [16] Chen et al, *PACS*, Volume 3, Issue 4, December 2015, Pages 143–150.
- [17] A. A. Oraevsky, S. Jacques, and F. Tittel, *Applied Optics* 36, 402–415 (1997).
- [18] Di Ninni P., Martelli F., Zaccanti G. 2011 *Phys. Med. Biol.* 56 N21.
- [19] ANSI, 136.1-2000 (The Laser Institute of America, 2000).
- [20] X. L. Dean-Ben, V. Ntziachristos and D. Razansky, *IEEE Transactions on Medical Imaging*, vol. 31, no. 5, pp. 1154-1162 (2012).
- [21] A. Chekkoury, J. Gateau, W. Driessen, P. Symvoulidis, N. Bézière, A. Feuchtinger, A. Walch, and V. Ntziachristos, *Biomed. Opt. Express* 6, 3134-3148 (2015).
- [22] Y. Han, L. Ding, X. Ben, D. Razansky, J. Prakash, and V. Ntziachristos, *Opt. Lett.* 42, 979-982 (2017).
- [23] Shaw CB, Prakash J, Pramanik M, Yalavarthy PK, *J. Biomed. Opt.*, vol. 18, (2013).

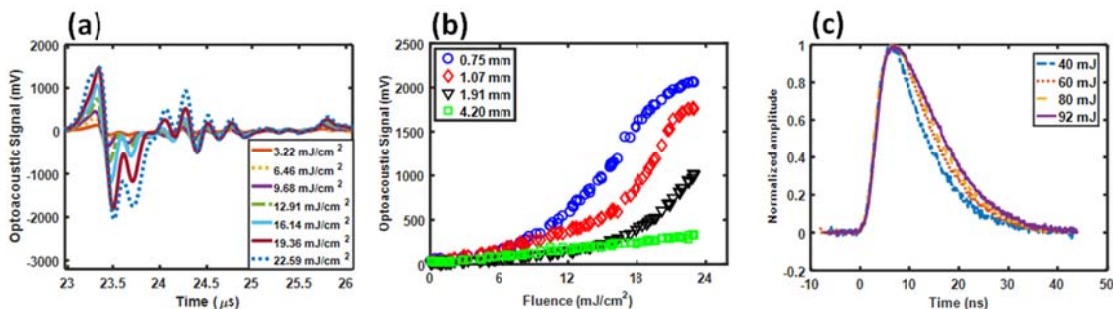


Figure 1. Raw optoacoustic signal from a mixture of ink, intralipid and agar phantom (MEAS-1) at different light fluence. (a) Raw optoacoustic data measured by the experimental setup. (b) Plot showing the absolute value of the optoacoustic signal at different depths 0.75, 1.07, 1.91, and 4.2 mm as a function of light fluence. (c) Laser pulse width measured with photodiode at different laser energies.

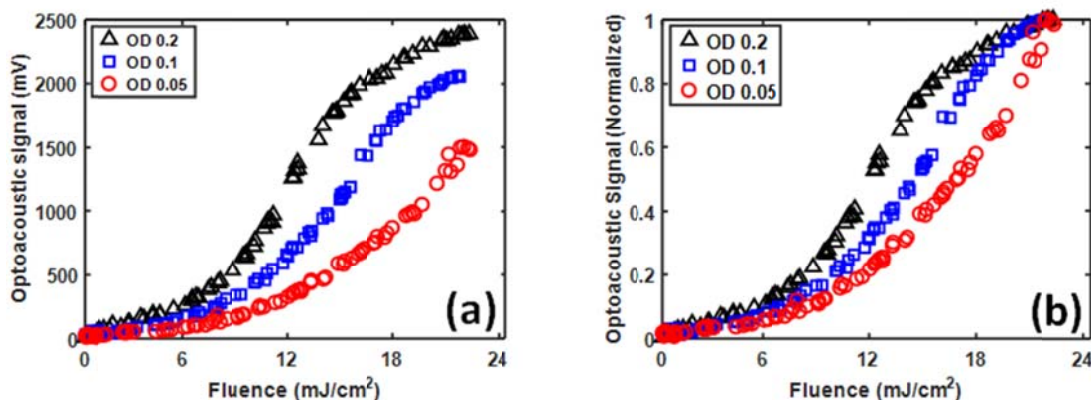


Figure 2. Optoacoustic signal variation over light fluence with different absorption concentration: (a) Variation of measured optoacoustic signal from a mixture of ink, intralipid and agar (MEAS-2) at different light fluence and with different optical densities (OD) of Ink. (b) Normalized optoacoustic signal variation of Figure 2(a).

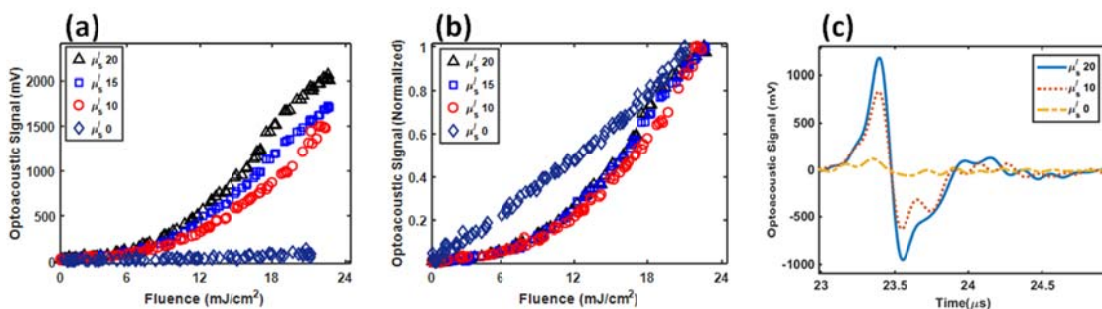


Figure 3. Optoacoustic Signal variation over light fluence at different scattering coefficient: (a) Variation of measured optoacoustic signal from a mixture of ink, intralipid and agar (MEAS-3) at different light fluence and with different reduced scattering coefficient (attained by varying Intralipid concentration). (b) Normalized optoacoustic signal variation of Figure 3(a). (c) Raw optoacoustic data for ink phantom with different reduced scattering coefficient acquired from measurement MEAS-3 when light fluence is 16 mJ/cm^2 .

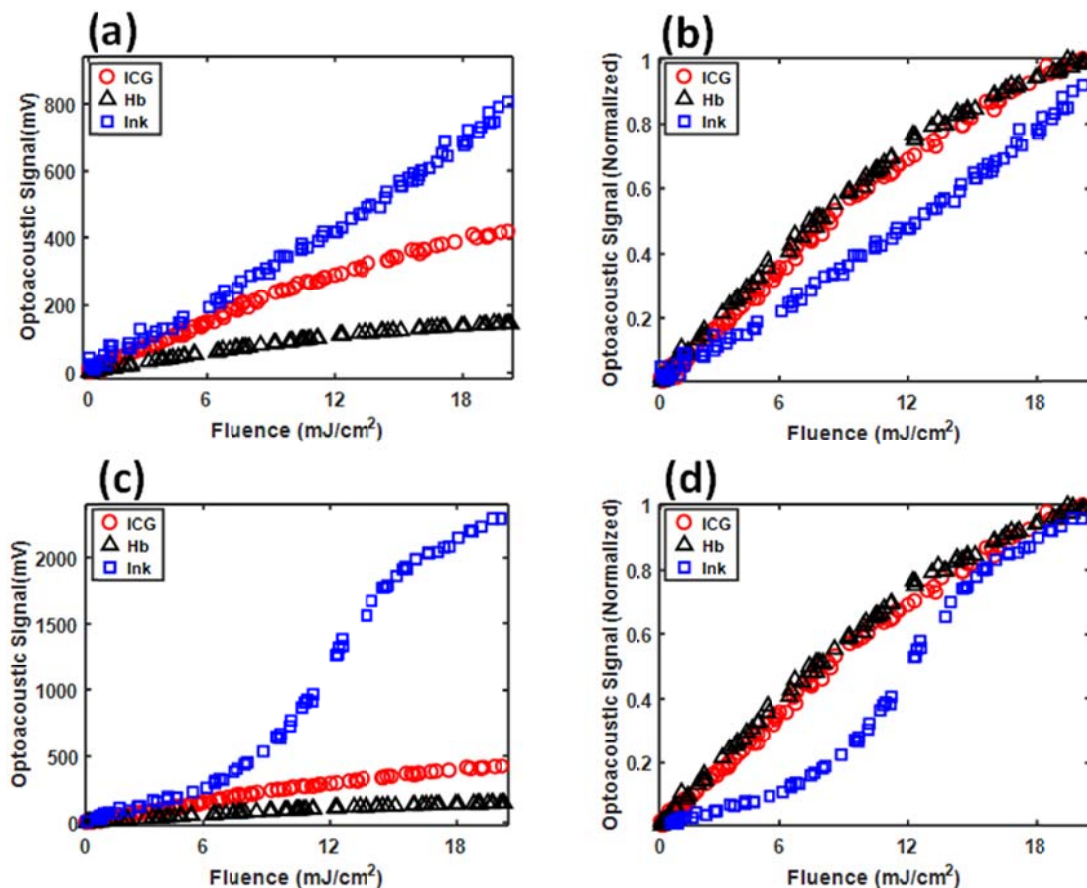


Figure 4. Optoacoustic signal variation over light fluence with different materials: (a) Variation of measured optoacoustic signal at different light fluence and with different materials (Hemoglobin, India Ink, Indocyanine Green (ICG)). There was no scattering in the media measured. (b) Normalized optoacoustic signal variation of Figure 4(a). (c) Variation of measured optoacoustic signal at different light fluence and with different materials with same absorption coefficient $\mu_a(r) = 0.23 \text{ cm}^{-1}$ at 800 nm and different reduced scattering coefficient, Hemoglobin (diluted mouse blood), India Ink ($\mu'_s(r) = 10$), Indocyanine Green ($\mu'_s(r) = 0$). (d) Normalized optoacoustic signal variation of Figure 4(c).

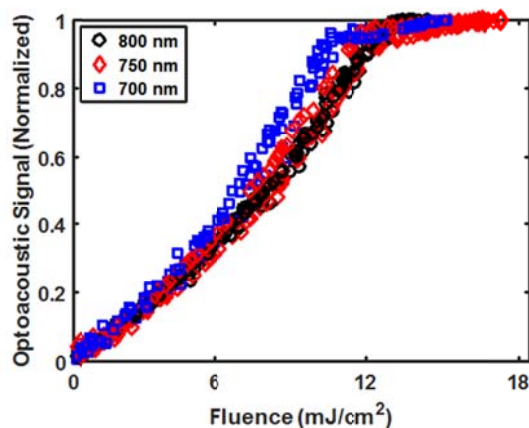


Figure 5. Strength of optoacoustic signal from ink phantoms at different light fluence and wavelengths (MEAS-5). The graph shows the results obtained at three different wavelengths, normalized to their respective maximum values.

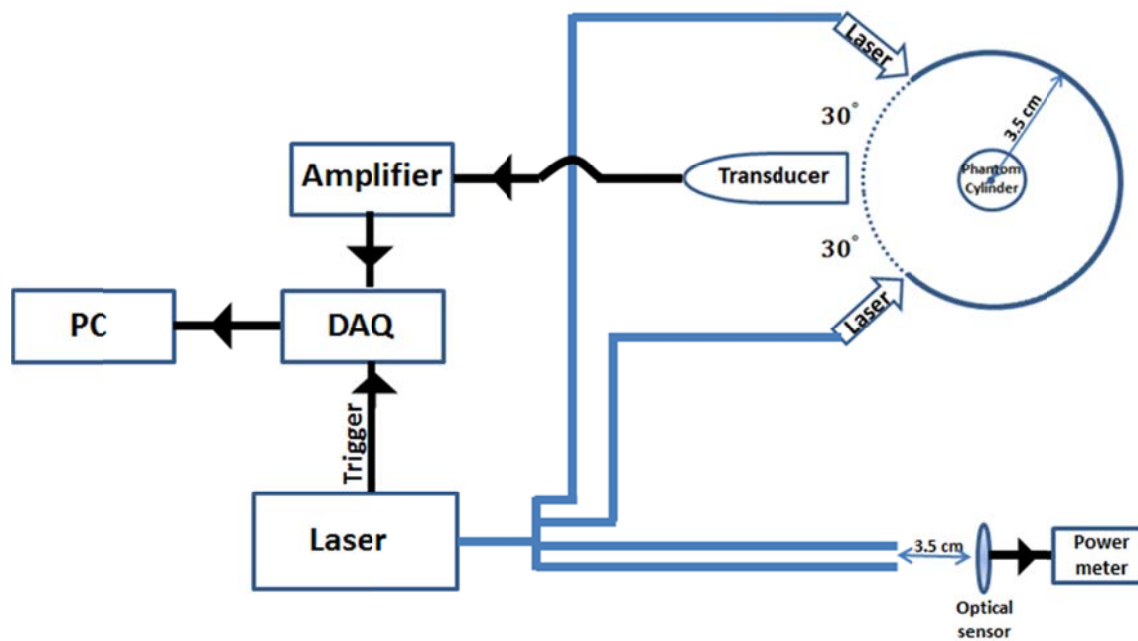


Figure 6. Schematic of the setup used for studying nonlinear optoacoustic effect.

Graphical Abstract

Non-linearity is observed in optoacoustic tomography in diffusive media by increasing light fluence. The non-linearity shows a piecewise linear function and there is a certain fluence threshold needed to trigger the transition from linear to non-linear regime. The optoacoustic signal shows prominent non-linearity by increasing absorption and scattering coefficient. Different materials can have different non-linear trend and the laser wavelength has effect on the trend.

